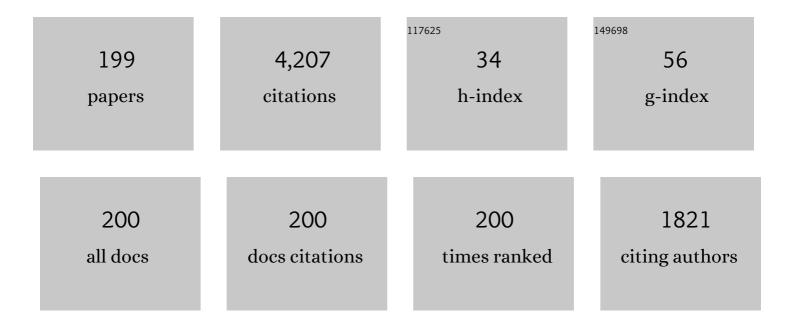
Guo-Sheng Xu

List of Publications by Year in descending order

Source: https://exaly.com/author-pdf/1675008/publications.pdf Version: 2024-02-01



#	Article	IF	CITATIONS
1	A long-pulse high-confinement plasma regime in the Experimental Advanced Superconducting Tokamak. Nature Physics, 2013, 9, 817-821.	16.7	234
2	First Evidence of the Role of Zonal Flows for the <mml:math xmlns:mml="http://www.w3.org/1998/Math/MathML" display="inline"><mml:mi>L</mml:mi><mml:mtext mathvariant="normal">â^²<mml:mi>H</mml:mi>Transition at Marginal Input Power in the EAST Tokamak. Physical Review Letters, 2011, 107, 125001.</mml:mtext </mml:math 	7.8	152
3	Physics Design of CFETR: Determination of the Device Engineering Parameters. IEEE Transactions on Plasma Science, 2014, 42, 495-502.	1.3	141
4	Spatio-temporal evolution of the L → l → H transition. Physics of Plasmas, 2012, 19, .	1.9	117
5	Magnetic Topology Changes Induced by Lower Hybrid Waves and their Profound Effect on Edge-Localized Modes in the EAST Tokamak. Physical Review Letters, 2013, 110, 235002.	7.8	112
6	Direct Measurement of Poloidal Long-WavelengthE×BFlows in the HT-7 Tokamak. Physical Review Letters, 2003, 91, 125001.	7.8	104
7	Overview of EAST experiments on the development of high-performance steady-state scenario. Nuclear Fusion, 2017, 57, 102019.	3.5	102
8	Turbulent-driven low-frequency shearedE×Bflows as the trigger for the H-mode transition. Nuclear Fusion, 2013, 53, 073053.	3.5	101
9	Advances in H-mode physics for long-pulse operation on EAST. Nuclear Fusion, 2015, 55, 104015.	3.5	101
10	Progress of long pulse and H-mode experiments in EAST. Nuclear Fusion, 2013, 53, 104006.	3.5	100
11	New Edge Coherent Mode Providing Continuous Transport in Long-Pulse H-mode Plasmas. Physical Review Letters, 2014, 112, 185004.	7.8	93
12	New Steady-State Quiescent High-Confinement Plasma in an Experimental Advanced Superconducting Tokamak. Physical Review Letters, 2015, 114, 055001.	7.8	93
13	Recent advances in EAST physics experiments in support of steady-state operation for ITER and CFETR. Nuclear Fusion, 2019, 59, 112003.	3.5	93
14	Study on H-mode access at low density with lower hybrid current drive and lithium-wall coatings on the EAST superconducting tokamak. Nuclear Fusion, 2011, 51, 072001.	3.5	91
15	Zonal flow triggers the L-H transition in the Experimental Advanced Superconducting Tokamak. Physics of Plasmas, 2012, 19, 072311.	1.9	83
16	Blob/hole formation and zonal-flow generation in the edge plasma of the JET tokamak. Nuclear Fusion, 2009, 49, 092002.	3.5	81
17	Upgrade of Langmuir probe diagnostic in ITER-like tungsten mono-block divertor on experimental advanced superconducting tokamak. Review of Scientific Instruments, 2016, 87, 083504.	1.3	80
18	Fast reciprocating probe system on the EAST superconducting tokamak. Review of Scientific Instruments, 2010, 81, 113501.	1.3	59

#	Article	IF	CITATIONS
19	Approaches towards long-pulse divertor operations on EAST by active control of plasma–wall interactions. Nuclear Fusion, 2014, 54, 013002.	3.5	54
20	Characterizations of power loads on divertor targets for type-I, compound and small ELMs in the EAST superconducting tokamak. Nuclear Fusion, 2013, 53, 073028.	3.5	51
21	Integration of full divertor detachment with improved core confinement for tokamak fusion plasmas. Nature Communications, 2021, 12, 1365.	12.8	50
22	Observation of Cocurrent Toroidal Rotation in the EAST Tokamak with Lower-Hybrid Current Drive. Physical Review Letters, 2011, 106, 235001.	7.8	46
23	Realization of minute-long steady-state H-mode discharges on EAST. Plasma Science and Technology, 2017, 19, 032001.	1.5	46
24	Improvement of divertor triple probe system and its measurements under full graphite wall on EAST. Fusion Engineering and Design, 2009, 84, 57-63.	1.9	44
25	Particle and power deposition on divertor targets in EAST H-mode plasmas. Nuclear Fusion, 2012, 52, 063024.	3.5	44
26	Promising High-Confinement Regime for Steady-State Fusion. Physical Review Letters, 2019, 122, 255001.	7.8	43
27	Investigation of lower hybrid wave coupling and current drive experiments at different configurations in experimental advanced superconducting tokamak. Physics of Plasmas, 2011, 18, .	1.9	42
28	Simulation of transition dynamics to high confinement in fusion plasmas. Physics Letters, Section A: General, Atomic and Solid State Physics, 2015, 379, 3097-3101.	2.1	39
29	Intermittent convective transport carried by propagating electromagnetic filamentary structures in nonuniformly magnetized plasma. Physics of Plasmas, 2010, 17, 022501.	1.9	38
30	Numerical modeling of the transition from low to high confinement in magnetically confined plasma. Plasma Physics and Controlled Fusion, 2016, 58, 014031.	2.1	38
31	Observation of Confined Current Ribbon in JET Plasmas. Physical Review Letters, 2010, 104, 185003.	7.8	37
32	Divertor impurity seeding with a new feedback control scheme for maintaining good core confinement in grassy-ELM H-mode regime with tungsten monoblock divertor in EAST. Nuclear Fusion, 2020, 60, 086001.	3.5	37
33	Scaling of divertor power footprint width in RF-heated type-III ELMy H-mode on the EAST superconducting tokamak. Nuclear Fusion, 2014, 54, 114002.	3.5	36
34	Numerical simulations of blobs with ion dynamics. Plasma Physics and Controlled Fusion, 2017, 59, 025012.	2.1	35
35	Advances in plasma–wall interaction control for H-mode operation over 100 s with ITER-like tungsten divertor on EAST. Nuclear Fusion, 2019, 59, 086036.	3.5	35
36	Dynamics of L–H transition and I-phase in EAST. Nuclear Fusion, 2014, 54, 103002.	3.5	33

#	Article	IF	CITATIONS
37	Progress toward steady-state tokamak operation exploiting the high bootstrap current fraction regime. Physics of Plasmas, 2016, 23, .	1.9	33
38	Suppression of edge localized modes with real-time boron injection using the tungsten divertor in EAST. Nuclear Fusion, 2021, 61, 014002.	3.5	33
39	Integrated Operating Scenario to Achieve 100-Second, High Electron Temperature Discharge on EAST. Plasma Science and Technology, 2016, 18, 457-459.	1.5	32
40	Divertor detachment and asymmetry in H-mode operation with an ITER-like tungsten divertor in EAST. Nuclear Fusion, 2019, 59, 126046.	3.5	26
41	Spatio-temporal evolution of the L → H and H → L transitions. Nuclear Fusion, 2013, 53, 073044.	3.5	25
42	Recent advances in long-pulse high-confinement plasma operations in Experimental Advanced Superconducting Tokamak. Physics of Plasmas, 2014, 21, 056107.	1.9	25
43	Experimental investigation of the interaction of IBW and LHCD in the HT-7 tokamak. Nuclear Fusion, 2004, 44, 400-405.	3.5	24
44	New dual gas puff imaging system with up-down symmetry on experimental advanced superconducting tokamak. Review of Scientific Instruments, 2012, 83, 123506.	1.3	24
45	On physical interpretation of two dimensional time-correlations regarding time delay velocities and eddy shaping. Physics of Plasmas, 2012, 19, .	1.9	24
46	Statistical characterization of turbulence in the boundary plasma of EAST. Plasma Physics and Controlled Fusion, 2013, 55, 115007.	2.1	24
47	Investigation of energy transport in DIII-D High- <i>β</i> _P EAST-demonstration discharges with the TGLF turbulent and NEO neoclassical transport models. Nuclear Fusion, 2017, 57, 036018.	3.5	23
48	Comparison of divertor behavior and plasma confinement between argon and neon seeding in EAST. Nuclear Fusion, 2021, 61, 066013.	3.5	23
49	In search of zonal flows using cross-bispectrum analysis in the boundary plasma of the Hefei Tokamak-7. Physics of Plasmas, 2002, 9, 150-154.	1.9	22
50	Divertor asymmetry and scrape-off layer flow in various divertor configurations in Experimental Advanced Superconducting Tokamak. Physics of Plasmas, 2012, 19, .	1.9	22
51	Status of neutron diagnostics on the experimental advanced superconducting tokamak. Review of Scientific Instruments, 2016, 87, 11D820.	1.3	22
52	A stationary long-pulse ELM-absent H-mode regime in EAST. Nuclear Fusion, 2017, 57, 086041.	3.5	22
53	Fast electron flux driven by lower hybrid wave in the scrape-off layer. Physics of Plasmas, 2015, 22, .	1.9	21
54	Stationary high-performance grassy ELM regime in EAST. Nuclear Fusion, 2020, 60, 076012.	3.5	21

#	Article	IF	CITATIONS
55	Advances in the high bootstrap fraction regime on DIII-D towards the <i>Q</i> =  5 mission of I state. Nuclear Fusion, 2017, 57, 056008.	TER_steady	20
56	First Evidence of Local <mml:math <br="" xmlns:mml="http://www.w3.org/1998/Math/MathML">display="inline"><mml:mi mathvariant="bold">E</mml:mi><mml:mo>×</mml:mo><mml:mi mathvariant="bold">B</mml:mi </mml:math> Drift in the Divertor Influencing the Structure and Stability of Confined Plasma near the Edge of Fusion Devices. Physical Review Letters, 2020, 124, 195002.	7.8	20
57	Study on the L–H transition power threshold with RF heating and lithium-wall coating on EAST. Nuclear Fusion, 2016, 56, 056013.	3.5	19
58	Experimental study on the magnetic coherent mode in the H-mode pedestal of EAST. Nuclear Fusion, 2018, 58, 112004.	3.5	19
59	Observation of nonlinear couplings between coexisting kinetic geodesic acoustic modes in the edge plasmas of the HT-7 tokamak. Nuclear Fusion, 2013, 53, 113008.	3.5	18
60	Edge-coherent-mode nature of the small edge localized modes in Experimental Advanced Superconducting Tokamak. Physics of Plasmas, 2014, 21, 092511.	1.9	18
61	Analysis of performance degradation in an electron heating dominant H-mode plasma after ECRH termination in EAST. Nuclear Fusion, 2018, 58, 066011.	3.5	18
62	Observation of a new turbulence-driven limit-cycle state in H-modes with lower hybrid current drive and lithium-wall conditioning in the EAST superconducting tokamak. Nuclear Fusion, 2012, 52, 123011.	3.5	17
63	Geometry and Physics Design of Lower Divertor Upgrade in EAST. IEEE Transactions on Plasma Science, 2018, 46, 1412-1416.	1.3	17
64	Design of EAST lower divertor by considering target erosion and tungsten ion transport during the external impurity seeding. Nuclear Fusion, 2021, 61, 066004.	3.5	17
65	Turbulence and transport studies in the edge plasma of the HT-7 tokamak. Nuclear Fusion, 2001, 41, 1835-1845.	3.5	16
66	Low-to-High Confinement Transition Mediated by Turbulence Radial Wave Number Spectral Shift in a Fusion Plasma. Physical Review Letters, 2016, 116, 095002.	7.8	16
67	Upgrade Design of Lower Divertor Langmuir Probe Diagnostic System in the EAST Tokamak. IEEE Transactions on Plasma Science, 2018, 46, 1331-1337.	1.3	16
68	Experimental study of detachment density threshold in L-mode plasmas on EAST. Plasma Physics and Controlled Fusion, 2020, 62, 065008.	2.1	16
69	Experimental Evidence of Intrinsic Current Generation by Turbulence in Stationary Tokamak Plasmas. Physical Review Letters, 2022, 128, 085003.	7.8	16
70	Recent progress on steady-state high-performance plasma research in the Hefei Tokamak-7. Physics of Plasmas, 2004, 11, 2543-2550.	1.9	15
71	Bifurcation analysis and dimension reduction of a predator-prey model for the L-H transition. Physics of Plasmas, 2013, 20, 102302.	1.9	15
72	Study of the L–l–H transition with a new dual gas puff imaging system in the EAST superconducting tokamak. Nuclear Fusion, 2014, 54, 013007.	3.5	15

#	Article	IF	CITATIONS
73	Scenario development for highβplow torque plasma withqminabove 2 and large-radius internal transport barrier in DIII-D. Nuclear Fusion, 2017, 57, 022016.	3.5	15
74	First observation of a new zonal-flow cycle state in the H-mode transport barrier of the experimental advanced superconducting Tokamak. Physics of Plasmas, 2012, 19, 122502.	1.9	14
75	Evidence and modeling of 3D divertor footprint induced by lower hybrid waves on EAST with tungsten divertor operations. Nuclear Fusion, 2017, 57, 126054.	3.5	14
76	Experimental study of heating scheme effect on the inner divertor power footprint widths in EAST lower single null discharges. Plasma Physics and Controlled Fusion, 2018, 60, 045001.	2.1	14
77	Hot spots induced by LHCD in the shadow of antenna limiters in the EAST tokamak. Physics of Plasmas, 2018, 25, .	1.9	14
78	Advances in physics understanding of high poloidal beta regime toward steady-state operation of CFETR. Physics of Plasmas, 2021, 28, .	1.9	14
79	Recent Progress on EAST. Fusion Science and Technology, 2013, 64, 417-423.	1.1	13
80	Effect of â^‡ <i>B drift</i> on the H-mode power threshold in upper single null plasmas with ITER-like tungsten divertor on EAST. Physics of Plasmas, 2018, 25, .	1.9	13
81	Grassy ELM regime at low pedestal collisionality in high-power tokamak plasma. Nuclear Fusion, 2021, 61, 016032.	3.5	13
82	A Dip Structure in the Intrinsic Toroidal Rotation Near the Edge of the Ohmic Plasmas in EAST. Plasma Science and Technology, 2011, 13, 397-404.	1.5	12
83	Characteristics of edge-localized modes in the experimental advanced superconducting tokamak (EAST). Plasma Physics and Controlled Fusion, 2012, 54, 095003.	2.1	12
84	Observation of a quasi-coherent high-frequency electromagnetic mode at the pedestal region in EAST RF-dominant H-modes. Nuclear Fusion, 2014, 54, 043014.	3.5	12
85	Edge multi-energy soft x-ray diagnostic in Experimental Advanced Superconducting Tokamak. Review of Scientific Instruments, 2015, 86, 123512.	1.3	12
86	One-dimensional modelling of limit-cycle oscillation and H-mode power scaling. Nuclear Fusion, 2015, 55, 053029.	3.5	12
87	Effort of lower hybrid current drive experiments toward to H-mode in EAST. Nuclear Fusion, 2017, 57, 022022.	3.5	12
88	Statistical study of particle flux footprint widths with tungsten divertor in EAST. Plasma Physics and Controlled Fusion, 2019, 61, 045001.	2.1	12
89	Multiscale coherent structures in tokamak plasma turbulence. Physics of Plasmas, 2006, 13, 102509.	1.9	11
90	Effect of magnetic geometry on divertor asymmetry and access to high confinement mode in EAST. Journal of Nuclear Materials, 2013, 438, S280-S284.	2.7	11

#	Article	IF	CITATIONS
91	Observations of the effect of lower hybrid waves on ELM behaviour in EAST. Nuclear Fusion, 2015, 55, 033012.	3.5	11
92	Retarding field analyzer for the EAST plasma boundary. Review of Scientific Instruments, 2016, 87, 123503.	1.3	11
93	Experimental observation of coexisting electromagnetic fluctuations correlating with the inter-ELM pedestal evolution on EAST. Physics of Plasmas, 2019, 26, .	1.9	11
94	Overview of the ICRF antenna coupling experiments on EAST. Nuclear Fusion, 2021, 61, 035001.	3.5	11
95	Langmuir-magnetic probe measurements of ELMs and dithering cycles in the EAST tokamak. Plasma Physics and Controlled Fusion, 2014, 56, 095023.	2.1	10
96	Enhanced-recycling H-mode regimes with edge coherent modes achieved by RF heating with lithium-wall conditioning in the EAST superconducting tokamak. Nuclear Fusion, 2014, 54, 124001.	3.5	10
97	Simulations of Ar seeding by SOLPS-ITER for a slot-type divertor concept. Physics of Plasmas, 2020, 27, 062509.	1.9	10
98	Experimental observation of the localized coupling between geodesic acoustic mode and magnetic islands in tokamak plasmas. Nuclear Fusion, 2021, 61, 036034.	3.5	10
99	Divertor detachment with neon seeding in grassy-ELM H-mode in EAST. Plasma Physics and Controlled Fusion, 2020, 62, 095025.	2.1	10
100	Power law fitting of the ion saturation current and the three-temperature Maxwellian EEDF in a multi-dipole confined hot cathode discharge: an experimental revisitation. Plasma Sources Science and Technology, 2022, 31, 045002.	3.1	10
101	Recent progress in Chinese fusion research based on superconducting tokamak configuration. Innovation(China), 2022, 3, 100269.	9.1	10
102	Edge turbulent transport with lower hybrid current drive in the Hefei Tokamak-7. Physics of Plasmas, 2004, 11, 207-213.	1.9	9
103	Observation of Blobs and Holes in the Boundary Plasma of EAST Tokamak. Plasma Science and Technology, 2011, 13, 410-414.	1.5	9
104	Velocimetry of edge turbulence during the dithering L–H transition with dynamic programming based time-delay estimation technique in the EAST superconducting tokamak. Plasma Physics and Controlled Fusion, 2013, 55, 105006.	2.1	9
105	Influence of helium puff on divertor asymmetry in Experimental Advanced Superconducting Tokamak. Physics of Plasmas, 2014, 21, 022509.	1.9	9
106	Understanding L–H transition in tokamak fusion plasmas. Plasma Science and Technology, 2017, 19, 033001.	1.5	9
107	The effects of magnetic topology on the scrape-off layer turbulence transport in the first divertor plasma operation of Wendelstein 7-X using a new combined probe. Nuclear Fusion, 2019, 59, 066001.	3.5	9
108	Progress of Divertor Heat and Particle Flux Control in EAST for Advanced Steady-State Operation in the Last 10 Years. Journal of Fusion Energy, 2021, 40, 1.	1.2	9

#	Article	IF	CITATIONS
109	Observation of fully detached divertor integrated with improved core confinement for tokamak fusion plasmas. Physics of Plasmas, 2021, 28, .	1.9	9
110	Effect of gas puffing from different side on lower hybrid wave-plasma coupling in experimental advanced superconductive tokamak. Physics of Plasmas, 2013, 20, 102504.	1.9	8
111	Preliminary study of divertor particle exhaust in the EAST superconducting tokamak. Plasma Science and Technology, 2017, 19, 095101.	1.5	8
112	Experimental study on low recycling no-ELM high confinement mode in EAST. Nuclear Fusion, 2019, 59, 086044.	3.5	8
113	Characteristics of off-axis sawteeth with an internal transport barrier in EAST. Nuclear Fusion, 2019, 59, 084005.	3.5	8
114	A non-axisymmetric <i>E</i> × <i>B</i> shear inducing toroidally localized turbulence with a magnetic perturbation field in EAST. Nuclear Fusion, 2020, 60, 016020.	n _{3.5} plied	8
115	Automated electron temperature fitting of Langmuir probe l–V trace in plasmas with multiple Maxwellian EEDFs. Plasma Science and Technology, 2020, 22, 085404.	1.5	8
116	Design of quasi-axisymmetric stellarators with varying-thickness permanent magnets based on Fourier and surface magnetic charges method. Nuclear Fusion, 2021, 61, 026025.	3.5	8
117	Plasma performance improvement with favourable B t relative to unfavourable B t in RF-heated H-mode plasmas in EAST. Nuclear Fusion, 2021, 61, 026014.	3.5	8
118	Effects of radial transport on divertor power and particle flux widths under different operational regimes in EAST. Nuclear Fusion, 2021, 61, 106015.	3.5	8
119	Development of Langmuir probe array for the new lower tungsten divertor in EAST. Fusion Engineering and Design, 2022, 175, 113011.	1.9	8
120	Application of wavelet multiresolution analysis to the study of self-similarity and intermittency of plasma turbulence. Review of Scientific Instruments, 2006, 77, 083505.	1.3	7
121	Real-time measurements for edge plasma parameters using triple probes on EAST. Physica Scripta, 2008, 78, 035501.	2.5	7
122	Estimation of Neutral Density in Edge Plasma with Double Null Configuration in EAST. Plasma Science and Technology, 2011, 13, 431-434.	1.5	7
123	Small amplitude oscillations before the L-H transition in EAST. Plasma Physics and Controlled Fusion, 2018, 60, 035012.	2.1	7
124	Investigation of impurity confinement in lower hybrid wave heated plasma on EAST tokamak. Nuclear Fusion, 2018, 58, 016001.	3.5	7
125	Modeling the effect of divertor closure on plasma detachment for new divertor design of EAST by SOLPS. Plasma Physics and Controlled Fusion, 2019, 61, 095007.	2.1	7
126	Measurement of edge electron density profile with lithium beam emission spectroscopy (Li-BES) diagnostic on the experimental advanced superconducting tokamak (EAST). Fusion Engineering and Design, 2019, 144, 133-140.	1.9	7

#	Article	IF	CITATIONS
127	Investigation of multifaceted asymmetric radiation from the edge (MARFE) with impurity injection from the upper divertor on the Experimental Advanced Superconducting Tokamak. Plasma Physics and Controlled Fusion, 2020, 62, 075005.	2.1	7
128	DesignÂof quasi-axisymmetric stellarators with variable-thickness perpendicular permanent magnets based on a two-step magnet designÂstrategy. Nuclear Fusion, 2021, 61, 106028.	3.5	7
129	Simultaneous ion temperature and flow measurements using a retarding field analyzer in the HL-2A tokamak. Radiation Effects and Defects in Solids, 2013, 168, 776-788.	1.2	6
130	First measurements of Hiro currents in vertical displacement event in tokamaks. Physics of Plasmas, 2015, 22, 060702.	1.9	6
131	Study of power width scaling in scrape-off layer with 2D electrostatic turbulence code based on EAST L-mode discharges. Physics of Plasmas, 2019, 26, 042509.	1.9	6
132	Edge turbulence characteristics and transport during the ELM mitigation with <i>n</i> = 1 resonant magnetic perturbation on EAST. Nuclear Fusion, 2020, 60, 082001.	3.5	6
133	Characteristics of double-peaked particle deposition at divertor target plates in the EAST tokamak. Nuclear Fusion, 2021, 61, 096004.	3.5	6
134	Investigation of annular/central collapse events triggered by the double tearing modes in EAST. Nuclear Fusion, 2021, 61, 106008.	3.5	6
135	Reciprocating Probe Measurements of L-H Transition in LHCD H-Mode on EAST. Plasma Science and Technology, 2013, 15, 619-622.	1.5	5
136	Effects of heating power on divertor in-out asymmetry and scrape-off layer flow in reversed field on Experimental Advanced Superconducting Tokamak. Physics of Plasmas, 2014, 21, 122514.	1.9	5
137	Lower hybrid current drive and ion cyclotron range of frequencies heating experiments in H-mode plasmas in Experimental Advanced Superconducting Tokomak. Physics of Plasmas, 2014, 21, 061501.	1.9	5
138	Active control of divertor heat and particle fluxes in EAST towards advanced steady state operations. Journal of Nuclear Materials, 2015, 463, 99-103.	2.7	5
139	Stability analysis of ELMs in long-pulse discharges with ELITE code on EAST tokamak. Plasma Physics and Controlled Fusion, 2018, 60, 055002.	2.1	5
140	Observation of tungsten impurities induced 2/1 snake fluctuations and their interactions with discrete double BAE pairs on EAST. Nuclear Fusion, 2018, 58, 124004.	3.5	5
141	An experimental investigation of blob behaviors in lower hybrid wave dominant heating scenarios on EAST. Physics of Plasmas, 2019, 26, 072305.	1.9	5
142	Optimization of pumping performance in the EAST upgraded divertor. Plasma Physics and Controlled Fusion, 2019, 61, 065001.	2.1	5
143	Error analysis and cazlibration of Langmuir probes embedded in ITER-like tungsten divertor on EAST. Nuclear Materials and Energy, 2021, 27, 100996.	1.3	5
144	On the role of the hydrogen concentration in the L-H transition power threshold in EAST. Nuclear Fusion, 2021, 61, 016010.	3.5	5

#	Article	IF	CITATIONS
145	The influence of neutral particles on boundary turbulence and confinement in the HT-7 tokamak. Plasma Physics and Controlled Fusion, 2003, 45, 1805-1814.	2.1	4
146	Impact of E × B flow shear on turbulence and resulting power fall-off width in H-mode plasmas in experimental advanced superconducting tokamak. Physics of Plasmas, 2015, 22, 062504.	1.9	4
147	Modeling of advanced divertor configuration on experimental advanced superconducting tokamak by SOLPS5.0/B2.5-Eirene. Physics of Plasmas, 2016, 23, .	1.9	4
148	Visible imaging measurement of position and displacement of the last closed flux surface in EAST tokamak. Fusion Engineering and Design, 2017, 119, 42-50.	1.9	4
149	E × B flow shear drive of the linear low- <i>n</i> modes of EHO in the QH-m Nuclear Fusion, 2017, 57, 086047.	iod <u>ę r</u> egim	e. ₄
150	Comparison of measurements with different types of divertor Langmuir probe in EAST tokamak. Journal of Instrumentation, 2019, 14, P06028-P06028.	1.2	4
151	Tomographic reconstruction of emissive profile in the divertor region for the visible light imaging diagnostic on Experimental Advanced Superconducting Tokamak. Fusion Engineering and Design, 2021, 163, 112149.	1.9	4
152	The impact of ELM mitigation on tungsten source in the EAST divertor. Nuclear Fusion, 2021, 61, 046046.	3.5	4
153	Impact of divertor closure on edge plasma behavior in EAST H-mode plasmas. Plasma Physics and Controlled Fusion, 2021, 63, 065004.	2.1	4
154	Type-I ELM mitigation by continuous lithium granule gravitational injection into the upper tungsten divertor in EAST. Nuclear Fusion, 2021, 61, 066022.	3.5	4
155	Experimental study of the influence of gas puff locations on H-mode boundary plasmas with argon seeding on EAST. Plasma Physics and Controlled Fusion, 2021, 63, 085001.	2.1	4
156	Enhancement of edge turbulence concomitant with ELM suppression during boron powder injection in EAST. Physics of Plasmas, 2021, 28, 082512.	1.9	4
157	Tungsten control in type-I ELMy H-mode plasmas on EAST. Nuclear Science and Techniques/Hewuli, 2021, 32, 1.	3.4	4
158	Study on the divertor plasma behavior through sweeping strike point in the new lower divertor on EAST. Chinese Physics B, 0, , .	1.4	4
159	Development of advanced stellarator with identical permanent magnet blocks. Cell Reports Physical Science, 2022, 3, 100709.	5.6	4
160	Plasma electron temperature measurement in a Mather-type plasma focus filled with hydrogen by a continuum intensity analysis. Plasma Devices and Operations, 2004, 12, 31-38.	0.6	3
161	Extraction of large-scale coherent structure from plasma turbulence using rake probe and wavelet analysis in a tokamak. Review of Scientific Instruments, 2006, 77, 063505.	1.3	3
162	Analysis of electron temperature, impurity transport and MHD activity with multi-energy soft x-ray diagnostic in EAST tokamak. Plasma Science and Technology, 2017, 19, 125101.	1.5	3

#	Article	IF	CITATIONS
163	Power Modulation System and Experiments of Lower Hybrid Wave on EAST. IEEE Access, 2018, 6, 37413-37417.	4.2	3
164	Comparison of natural grassy ELM behavior in favorable/unfavorable B t in EAST. Plasma Science and Technology, 2021, 23, 095105.	1.5	3
165	A simple replacement of tungsten filament hot cathodes by DC heated LaB6 rod and its noise characteristics with laser-induced fluorescence. Review of Scientific Instruments, 2021, 92, 123503.	1.3	3
166	<scp>Influence</scp> of the drifts on the doubleâ€peaked emission profile of the visible light in the upper divertor region of <scp>EAST</scp> . Contributions To Plasma Physics, 2022, 62, .	1.1	3
167	Boundary plasma behavior under different wall conditions on HT-7 tokamak. Journal of Nuclear Materials, 2003, 313-316, 259-262.	2.7	2
168	Edge plasma modelling for HT-7 superconducting tokamak experiments. Journal of Nuclear Materials, 2007, 363-365, 544-549.	2.7	2
169	Study of Scrape-Off-Layer Width in Ohmic and Lower Hybrid Wave Heated Double-Null Divertor Plasma in EAST. Plasma Science and Technology, 2011, 13, 435-439.	1.5	2
170	Investigation on LHW-plasma coupling in H-mode plasma in EAST. , 2014, , .		2
171	Design of Langmuir probe diagnostic system for the upgraded lower tungsten divertor in EAST tokamak. Review of Scientific Instruments, 2018, 89, 10J127.	1.3	2
172	Combined Langmuir-magnetic probe measurements of type-I ELMy filaments in the EAST tokamak. Plasma Science and Technology, 2018, 20, 065101.	1.5	2
173	Pace making of edge localized modes with low-hybrid-wave power pulses in the EAST superconducting tokamak. Plasma Physics and Controlled Fusion, 2019, 61, 065023.	2.1	2
174	Statistical characteristics of the SOL turbulence in the first divertor plasma operation of W7-X using a reciprocating probe. Physics of Plasmas, 2020, 27, 122504.	1.9	2
175	Diamond-Coated Plasma Probes for Hot and Hazardous Plasmas. Materials, 2020, 13, 4524.	2.9	2
176	Comparison of dynamical features between the fast H-L and the H-I-L transition for EAST RF-heated plasmas. Physica Scripta, 2022, 97, 015601.	2.5	2
177	Fast-sweeping Langmuir probes: what happens to the I –V trace when sweeping frequency is higher than the ion plasma frequency?. Plasma Science and Technology, 2022, 24, 025404.	1.5	2
178	Development and application of limiter Langmuir probe array in EAST. Fusion Engineering and Design, 2022, 180, 113162.	1.9	2
179	Effects of edge-localized mode-induced neoclassical toroidal viscosity torque on the toroidal intrinsic rotation in the EAST tokamak. Radiation Effects and Defects in Solids, 2013, 168, 873-880.	1.2	1
180	Turbulence induced radial transport of toroidal momentum in boundary plasma of EAST tokamak. Physics of Plasmas, 2016, 23, .	1.9	1

#	Article	IF	CITATIONS
181	Upgrade of the multi-energy soft x-ray diagnostic system for studies of ELM dynamics in the EAST tokamak. Fusion Engineering and Design, 2018, 137, 414-419.	1.9	1
182	A new model of the L–H transition and H-mode power threshold. Plasma Science and Technology, 2018, 20, 094003.	1.5	1
183	Edge toroidal charge exchange spectra analysis in the EAST. Review of Scientific Instruments, 2018, 89, 10D103.	1.3	1
184	Observation of a fully non-inductive H-mode regime dominated by the sporadic-small edge-localized modes in EAST with a tungsten divertor. Plasma Physics and Controlled Fusion, 2019, 61, 085006.	2.1	1
185	Edge Toroidal Rotation Analysis by CXRS Diagnostic on EAST. Fusion Science and Technology, 2020, 76, 723-730.	1.1	1
186	Observation of direct power deposition of ICRF in EAST plasma boundary. Radiation Effects and Defects in Solids, 2021, 176, 1076-1091.	1.2	1
187	Divertor detachment operation in helium plasmas with ITER-like tungsten divertor in EAST. Plasma Science and Technology, 2022, 24, 075101.	1.5	1
188	Experimental investigation of scrape-off layer blob high density transition in L-mode plasmas on EAST. Plasma Science and Technology, 2022, 24, 075103.	1.5	1
189	Experimental investigation of electromagnetic GAMs under the influence of 3D magnetic topological structure in EAST. Plasma Physics and Controlled Fusion, 2022, 64, 054007.	2.1	1
190	Upgrade and application of the gas puff imaging system in EAST. Fusion Engineering and Design, 2022, 179, 113156.	1.9	1
191	Observation of non-thermal metastable ion velocity distributions in a miniaturized multi-dipole confined plasma device. Physics of Plasmas, 2022, 29, 063504.	1.9	1
192	Measurement of Reynolds Stress and Zonal Flows in a Tokamak Using Langmuir Probe Array. Contributions To Plasma Physics, 2006, 46, 455-459.	1.1	0
193	Electron thermal transport induced by magnetic turbulence in the HT-7 tokamak. Journal of Nuclear Materials, 2007, 363-365, 738-742.	2.7	0
194	Features of the repetition frequency of edge localized modes in EAST. Radiation Effects and Defects in Solids, 2012, 167, 743-751.	1.2	0
195	Innovative divertor concept development on DIII-D and EAST. , 2015, , .		0
196	L–H power threshold studies with tungsten/carbon divertor on the EAST tokamak. Radiation Effects and Defects in Solids, 2016, 171, 359-373.	1.2	0
197	The observation of field-aligned current during type-III ELM in EAST. Radiation Effects and Defects in Solids, 2017, 172, 555-566.	1.2	0
198	Linear simulation of magnetohydrodynamic plasma response to three-dimensional magnetic perturbations in high-l² _P plasmas. Nuclear Fusion, 2022, 62, 036022.	3.5	0

#	Article	IF	CITATIONS
199	Probabilistic effect of metastable excitation on lock-in amplified plasma laser-induced fluorescence diagnostics at modulation frequencies comparable to the fluorescence frequency. Journal of Plasma Physics, 2022, 88, .	2.1	О